

The Richness-Dependent Cluster Correlation Function: Early SDSS Data

Neta A. Bahcall¹, Feng Dong¹, Lei Hao¹, Paul Bode¹, Jim Annis², James E. Gunn¹,
Donald P. Schneider³

ABSTRACT

The cluster correlation function and its richness dependence are determined from 1108 clusters of galaxies – the largest sample of clusters studied so far – found in 379 deg² of Sloan Digital Sky Survey early data. The results are compared with previous samples of optically and X-ray selected clusters. The richness-dependent correlation function increases monotonically from an average correlation scale of $\sim 12 h^{-1}$ Mpc for poor clusters to $\sim 25 h^{-1}$ Mpc for the richer, more massive clusters with a mean separation of $\sim 90 h^{-1}$ Mpc. X-ray selected clusters suggest slightly stronger correlations than optically selected clusters ($\sim 2\text{-}\sigma$). The results are compared with large-scale cosmological simulations. The observed richness-dependent cluster correlation function is well represented by the standard flat LCDM model ($\Omega_m \simeq 0.3$, $h \simeq 0.7$), and is inconsistent with the considerably weaker correlations predicted by $\Omega_m = 1$ models. An analytic relation for the correlation scale versus cluster mean separation, $r_0 - d$, that best describes the observations and the LCDM prediction is $r_0 \simeq 2.6\sqrt{d}$ (for $d \simeq 20 - 90 h^{-1}$ Mpc). Data from the complete Sloan Digital Sky Survey, when available, will greatly enhance the accuracy of the results and allow a more precise determination of cosmological parameters.

Subject headings: cosmology:observations–cosmology:theory–cosmological parameters–dark matter–galaxies:clusters: general–large-scale structure of universe

¹Princeton University Observatory, Princeton, NJ 08544

²Fermi National Accelerator Laboratory, P.O. Box 500, Batavia, IL 60510

³Dept. of Astronomy and Astrophysics, The Pennsylvania State University, University Park, PA 16802

1. Introduction

The spatial correlation function of clusters of galaxies and its richness dependence provide powerful tests of cosmological models: both the amplitude of the correlation function and its dependence on cluster mass/richness are determined by the underlying cosmology. It has long been shown that clusters are more strongly correlated in space than galaxies, by an order-of-magnitude: the typical galaxy correlation scale, $\sim 5 h^{-1}$ Mpc, increases to $\sim 20 - 25 h^{-1}$ Mpc for the richest clusters (Bahcall & Soneira 1983; Klypin & Kopylov 1983; see also Bahcall 1988; Huchra et al. 1990; Postman, Huchra, & Geller 1992; Bahcall & West 1992; Peacock & West 1992; Dalton et al. 1994; Croft et al. 1997; Abadi, Lambas, & Muriel 1998; Lee & Park 1999; Borgani, Plionis, & Kolokotronis 1999; Collins et al. 2000; Gonzalez, Zaritsky, & Wechsler 2002; and references therein). Bahcall & Soneira (1983) showed that the cluster correlation function is richness dependent: the correlation strength increases with cluster richness, or mass. Many observations have since confirmed these results (references above), and theory has nicely explained them (Kaiser 1984; Bahcall & Cen 1992; Mo & White 1996; Governato et al. 1999; Colberg et al. 2000; Moscardini et al. 2000; Sheth, Mo, & Tormen 2001). But the uncertainties in the observed cluster correlation function as manifested by the scatter among different measurements remained large.

In this paper we use the largest sample of clusters yet investigated, 1108 clusters selected from 379 deg² of early Sloan Digital Sky Survey data (see the SDSS cluster catalog: Bahcall et al. 2003b), to determine the cluster correlation function. This large, complete sample of objectively selected clusters, ranging from poor to moderately rich systems in the redshift range $z = 0.1 - 0.3$, allows a new determination of the cluster correlation function and its richness dependence. We compare the SDSS cluster correlation function with results of previous optically and X-ray selected clusters (§3). We use large-scale cosmological simulations to compare the observational results with cosmological models (§4). The data are consistent with predictions from the standard flat LCDM model ($\Omega_m \sim 0.3$, $h \sim 0.7$), which best fits numerous other observations (e.g., Bahcall, Ostriker, Perlmutter, & Steinhardt 1999; Bennett et al. 2003; Spergel et al. 2003).

2. SDSS Cluster Selection

The Sloan Digital Sky Survey (SDSS; York et al. 2000) will provide a comprehensive digital imaging survey of 10⁴ deg² of the North Galactic Cap (and a smaller, deeper area in the South) in five bands (u, g, r, i, z) to a limiting magnitude of $r < 23$, followed by a spectroscopic multi-fiber survey of the brightest one million galaxies, to $r < 17.7$, with a median redshift of $z \sim 0.1$ (Fukugita et al. 1996; Gunn et al. 1998; Lupton et al. 2001; Hogg

et al. 2001; Strauss, et al. 2002). For more details of the SDSS see Smith et al. (2002); Stoughton et al. (2002); and Pier et al. (2003).

Cluster selection was performed on 379 deg² of SDSS commissioning data, covering the area $\alpha(2000) = 355^\circ$ to 56° and 145.3° to 236.0° at $\delta(2000) = -1.25^\circ$ to 1.25° (runs 94/125 and 752/756). The clusters studied here were selected from these imaging data using a color-magnitude maximum-likelihood Brightest Cluster Galaxy method (maxBCG; Annis et al. 2003). The clusters are described in the SDSS cluster catalog of Bahcall et al. (2003b). The maxBCG method selects clusters based on the well-known color-luminosity relation of the brightest cluster galaxy (BCG) and the E/S0 red ridgeline. The method provides a cluster richness estimate, N_{gal} (the number of E/S0 galaxies within $1 h^{-1}$ Mpc of the BCG that are fainter than the BCG and brighter than $M_i(\text{lim}) = -20.25$), and a cluster redshift estimate that maximizes the cluster likelihood (with $1-\sigma$ uncertainty of $\sigma_z = 0.014$ for $N_{gal} \geq 10$ and $\sigma_z = 0.01$ for $N_{gal} \geq 20$ clusters). We use all maxBCG clusters in the estimated redshift range $z_{est} = 0.1 - 0.3$ that are above a richness threshold of $N_{gal} \geq 10$ (corresponding to velocity dispersion $\gtrsim 350 \text{ km s}^{-1}$); the sample contains 1108 clusters. The selection function and false-positive detection rate for these clusters have been estimated from simulations and from visual inspection to be $\lesssim 10\%$ (Bahcall et al. 2003b).

3. The Cluster Correlation Function

The two-point spatial correlation function is determined by comparing the observed distribution of cluster pairs as a function of pair separation with the distribution of random catalogs in the same volume. The correlation function is estimated from the relation $\xi_{cc}(r) = F_{DD}(r)/F_{RR}(r) - 1$, where $F_{DD}(r)$ and $F_{RR}(r)$ are the frequencies of cluster-cluster pairs as a function of pair separation r in the data and in random catalogs, respectively. The random catalogs contain $\sim 10^3$ times the number of clusters in each data sample; the clusters are randomly positioned on the sky within the surveyed area. The redshifts of the random clusters follow the redshifts of the observed clusters in order to minimize possible selection effects with redshift. Comoving coordinates in a flat LCDM cosmology with $\Omega_m = 0.3$ and a Hubble constant of $H_0 = 100 h \text{ km s}^{-1} \text{ Mpc}^{-1}$ are used throughout.

The uncertainty in the estimated cluster redshifts ($\sigma_z = 0.01$ for $N_{gal} \geq 20$ clusters and $\sigma_z = 0.014$ for $N_{gal} \geq 10$ to ≥ 15 clusters; §2) causes a small smearing effect in the cluster correlations. We use Monte Carlo simulations to correct for this effect. We use simulations with a realistic cluster distribution with redshift and richness, convolve the clusters with the observed Gaussian scatter in redshift as given above, and determine the new convolved cluster correlation function. As expected, the redshift uncertainty causes a slight weakening of the

true correlation function, especially at small separations, due to the smearing effect of the redshift uncertainty. We determine the correction factor for this effect as a function of scale r from 10^2 Monte Carlo simulations for each sample. The correction factor (typically $\lesssim 20\%$) is then applied to the correlation function. An additional small correction factor due to false-positive detections is also determined from Monte Carlo simulations using the estimated false-positive detection rate of $10\% \pm 5\%$ for $N_{gal} \geq 10$ clusters, $5\% \pm 5\%$ for $N_{gal} \geq 13$, and $< 5\%$ for the richest clusters with $N_{gal} \geq 15$. The correlation function uncertainties are determined from the Monte Carlo simulations. Each simulation contains the same number of clusters as the relevant data sample. The final uncertainties include the statistical uncertainties and the uncertainties due to the small correction factors in the redshift and false-positive corrections.

The correlation function is determined for clusters with richness thresholds of $N_{gal} \geq 10$, ≥ 13 , ≥ 15 , and ≥ 20 . The space densities of these clusters, corrected for selection function and redshift uncertainty (Bahcall et al. 2003a), are 5.3×10^{-5} , 2.2×10^{-5} , 1.4×10^{-5} , and $0.5 \times 10^{-5} h^3 \text{ Mpc}^{-3}$ ($z_{est} = 0.1 - 0.3$). The correlation function of the four samples are presented in Figure 1 and Table 1. The best-fit power-law relation, $\xi(r) = (\frac{r}{r_0})^{-\gamma}$, derived for $r \lesssim 50 h^{-1} \text{ Mpc}$, is shown for each sample. The power-law slope γ has been treated both as a free parameter and as a fixed value ($\gamma = 2$). The difference in the correlation scale r_0 for these different slopes is small ($\lesssim 2\%$), well within the measured uncertainty.

The richness dependence of the cluster correlation function is shown in Figure 2; it is presented as the dependence of the correlation scale r_0 on the cluster mean separation d (Bahcall & Soneira 1983; Szalay & Schramm 1985; Bahcall 1988; Croft et al. 1997; Governato et al. 1999; Colberg et al. 2000). Samples with intrinsically larger mean separations correspond to lower intrinsic cluster abundances ($n_{cl} = d^{-3}$) and thus to higher cluster richness and mass (for complete samples). We compare our results with those of previous optically and X-ray selected cluster samples (Figure 2). These include the correlation function of Abell clusters (Bahcall & Soneira 1983; Peacock & West 1992; Richness class ≥ 1 ; Richness = 0 clusters are an incomplete sample and should not be included); APM clusters (Croft et al. 1997); Edinburgh-Durham clusters (EDCC; Nichol et al. 1992); Las-Campanas Distant Cluster Survey (LCDCS; Gonzalez, Zaritsky, & Wechsler 2002); galaxy groups (2dF; Zandivarez, Merchan, & Padilla 2003); and X-ray selected clusters (REFLEX: Collins et al. 2000; and XBACS: Abadi, Lambas, & Muriel 1998; Lee & Park 1999). A summary of the results is presented in Table 1. For proper comparison of different samples, we will use the same set of standard parameters in the relative $r_0 - d$ plot: redshift $z \sim 0$, correlation power-law slope $\gamma = 2$, and all scales are in comoving units in the LCDM cosmology. We discuss these below.

Most of the cluster samples are at small redshifts, $z \lesssim 0.1$ (Table 1). The only exceptions

are the SDSS clusters ($z \simeq 0.1 - 0.3$), and the LCDCS ($z \simeq 0.35 - 0.575$). To convert the results to $z \sim 0$ we use large-scale cosmological simulations of an LCDM model and determine the cluster correlation function and the $r_0 - d$ relation at different redshifts. Details of the simulations and cluster selection are given in Bode et al. (2001) (see also §4). The correlation function is determined following the same method used for the data. We find that while both r_0 and d increase with redshift for the same mass clusters, as expected, there is no significant change ($\lesssim 3\%$) in the $r_0 - d$ relation as the redshift changes from $z = 0$ to ~ 0.5 (for $d \sim 20 - 90 h^{-1}$ Mpc). In Figure 2 we plot the individual parameters r_0 and d at the sample’s measured redshift as listed in Table 1; the relative $r_0 - d$ relation remains essentially unchanged to $z \simeq 0$.

Most of the cluster correlation functions (Table 1) have a power-law slope in the range of $\sim 2 \pm 0.2$. The APM highest richness subsamples report steeper slopes (3.2, 2.8, 2.3); they also have the smallest number of clusters (17, 29, 58). The correlation scale r_0 is inversely correlated with the power-law slope; a steeper slope typically yields a smaller correlation scale. We use the APM best χ^2 fit for r_0 at $\gamma = 2$ (Croft et al. 1997) for these richest subsamples. Using cosmological simulations, we investigate the dependence of r_0 on the slope within the more typical observed range of 2 ± 0.2 . For the current range of mean separations d we find only a small change in r_0 ($\lesssim 5\%$) when the slope changes within this observed range. The X-ray cluster sample XBACS yields similar correlation scales for slopes ranging from ~ 1.8 to 2.5 (Abadi, Lambas, & Muriel 1998 and Lee & Park 1999). Similarly, the SDSS correlation scales are essentially the same when using a free slope fit (typically 1.7 to 2.1) or a fixed slope of 2. Since most of the observations are reported with a slope of 2, we adopt the latter as the standard slope for the results presented in Figure 2. The only correction applied is to the three highest richness APM subsamples; these are shown both with and without the correction. We also verify using cosmological simulations that the LCDCS sample at $z \sim 0.35 - 0.575$, with a slope of 2.15, has an $r_0 - d$ relation consistent with the standard set of parameters used in Figure 2 ($z \simeq 0$, $\gamma \simeq 2$).

Finally, we convert all scales (r_0 and d from Table 1) to the same $\Omega_m=0.3$ cosmology (LCDM). The effect of the cosmology on the observed $r_0 - d$ relation is small ($\lesssim 3\%$), partly due to the small redshifts, where the effect is small, but also because the cosmology affects both r_0 and d in the same way, thus minimizing the relative change in the $r_0 - d$ relation.

A comparison of all the results, including the minor corrections discussed above, is shown in Figure 2. Figure 2a presents both optically and X-ray selected clusters; Figure 2b includes only the optical samples. The richness-dependence of the cluster correlation function is apparent in Figure 2. The X-ray clusters suggest somewhat stronger correlations than the optical clusters, at a $\sim 2\text{-}\sigma$ level. Improved optical and X-ray samples should reduce

the scatter and help address this important comparison.

4. Comparison with Cosmological Simulations

We compare the results with large-scale cosmological simulations of a standard LCDM model ($\Omega_m = 0.3$, $h = 0.67$, $\sigma_8 = 0.9$), and a tilted SCDM model, TSCDM ($\Omega_m = 1$, $h = 0.5$, $n = 0.625$, $\sigma_8 = 0.5$). The TPM high-resolution large-volume simulations (Bode et al. 2001) used 1.34×10^8 particles with an individual particle mass of $6.2 \times 10^{11} h^{-1} M_\odot$; the periodic box size is $1000 h^{-1}$ Mpc for LCDM and $669 h^{-1}$ Mpc for TSCDM. The simulated clusters are ordered by their abundance based on cluster mass within $1.5 h^{-1}$ Mpc. The results of the cosmological simulations for the $r_0 - d$ relation of $z = 0$ clusters are presented by the two bands in Figure 2 (1- σ range). A correlation function slope of 2 was used in the analysis. We also show the simulations results of Colberg et al. (2000) for LCDM, and Governato et al. (1999) for a standard untilted SCDM ($\Omega_m = 1$, $h = 0.5$, $n = 1$, $\sigma_8 = 0.7$). The agreement among the simulations is excellent. As expected, the untilted SCDM model yields smaller r_0 's than the strongly tilted model; LCDM yields the strongest correlations.

We determine an analytic relation that approximates the observed and the LCDM $r_0 - d$ relation: $r_0 \simeq 2.6\sqrt{d}$ (for $20 \lesssim d \lesssim 90$; all scales are in h^{-1} Mpc). The observed richness-dependent cluster correlation function agrees well with the standard LCDM model. The correlation scales, and the $r_0 - d$ relation, increase as $\Omega_m h$ decreases and the spectrum shifts to larger scales. The $\Omega_m = 1$ models yield considerably weaker correlations than observed. This fact has of course been demonstrated earlier; in fact, the strength of the cluster correlation function and its richness dependence were among the first indications against the standard $\Omega_m = 1$ SCDM model (Bahcall & West 1992; Croft et al. 1997; Borgani, Plionis, & Kolokotronis 1999; Governato et al. 1999; Colberg et al. 2000; and references therein).

The scatter in the observed $r_0 - d$ relation among different samples is still large, especially when both the optical and X-ray selected samples are included. A high-precision determination of the cosmological parameters cannot therefore be achieved at this point.

5. Conclusions

We determine the cluster correlation function and its richness dependence using 1108 clusters of galaxies found in 379 deg² of early SDSS data. The cluster correlation function shows a clear richness dependence, with increasing correlation strength with cluster richness/mass. The results are combined with previous samples of optical and X-ray clusters,

and compared with cosmological simulations. We find that the richness-dependent cluster correlation function is consistent with predictions from the standard flat LCDM model ($\Omega_m = 0.3$, $h = 0.7$), and, as expected, inconsistent with the weaker correlations predicted by $\Omega_m = 1$ models. We derive an analytic relation for the correlation scale versus cluster mean separation relation that best describes the observations and the LCDM expectations: $r_0 \simeq 2.6\sqrt{d}$. X-ray selected clusters suggest somewhat stronger correlations than the optically selected clusters, at a $\sim 2\text{-}\sigma$ level.

Funding for the creation and distribution of the SDSS Archive has been provided by the Alfred P. Sloan Foundation, the Participating Institutions, NASA, the NSF, the U.S. Department of Energy, the Japanese Monbukagakusho, and the Max Planck Society. The SDSS Web site is <http://www.sdss.org/>. The SDSS is managed by the Astrophysical Research Consortium (ARC) for the Participating Institutions. The Participating Institutions are The University of Chicago, Fermilab, the Institute for Advanced Study, the Japan Participation Group, The Johns Hopkins University, Los Alamos National Laboratory, the Max-Planck-Institute for Astronomy (MPIA), the Max-Planck-Institute for Astrophysics (MPA), New Mexico State University, University of Pittsburgh, Princeton University, the United States Naval Observatory, and the University of Washington.

REFERENCES

- Abadi, M., Lambas, D., & Muriel, H. 1998, *ApJ*, 507, 526
- Annis, J., et al. 2003, in preparation.
- Bahcall, N. A. & Soneira, R. M. 1983, *ApJ*, 270, 20
- Bahcall, N. A. 1988, *ARA&A*, 26, 631
- Bahcall, N. A. & West, M. J. 1992, *ApJ*, 392, 419
- Bahcall, N. A. & Cen, R. 1992, *ApJ*, 398, L81
- Bahcall, N. A., Ostriker, J. P., Perlmutter, S., & Steinhardt, P. J. 1999, *Science*, 284, 1481
- Bahcall, N. A., Dong, F., Bode, P. et al. 2003a, *ApJ*, 585, 182
- Bahcall, N. A. et al. 2003b, *ApJS*, vol.148 (October 2003), astro-ph/0305202
- Bennett, C. L. et al. 2003, *ApJ*, in press
- Bode, P., Bahcall, N. A., Ford, E. B., & Ostriker, J. P., 2001, *ApJ*, 551, 15

- Borgani, S., Plionis, M., & Kolokotronis, V. 1999, MNRAS, 305, 866
- Colberg, J. M. et al. 2000, MNRAS, 319, 209
- Collins, C. et al. 2000, MNRAS, 319, 939
- Croft, R. A. C. et al. 1997, MNRAS, 291, 305
- Dalton, G. B. et al. 1994, MNRAS, 271, L47
- Fukugita, M. et al. 1996, AJ, 111, 1748
- Gonzalez, A. H., Zaritsky, D., Wechsler, R. H. 2002, ApJ, 571, 129
- Governato, F. et al. 1999, MNRAS, 307, 949
- Gunn, J. E. et al. 1998, AJ, 116, 3040
- Hogg, D. W. et al. 2001, AJ, 122, 2129
- Huchra, J., Henry, J. P., Postman, M., & Geller, M. 1990, ApJ, 365, 66
- Kaiser, N. 1984, ApJ, 284, L9
- Klypin, A. A. & Kopylov, A. I. 1983, Soviet Astron. Lett. 9, 41
- Lee, S., Park, C. 1999, JKAS, 32, 1
- Lupton, R., et al. 2001, ASP Conf. Ser.238, vol.10, 269
- Mo, H. J. & White, S. D. M. 1996, MNRAS, 282, 347
- Moscardini, L., Matarrese, S., Lucchin, F., Rosati, P. 2000, MNRAS, 316, 283
- Nichol, R. C., Collins, C. A., Guzzo, L., & Lumsden, S. L. 1992, MNRAS, 255, 21
- Peacock, J. A. & West, M. J. 1992, MNRAS, 259, 494
- Pier, J. R. et al. 2003, AJ, 125, 1559
- Postman, M., Huchra, J., & Geller, M. 1992, ApJ, 384, 404
- Sheth, R. K., Mo, H. J., Tormen, G. 2001, MNRAS, 323, 1
- Smith, J. A. et al. 2002, AJ, 123, 2121
- Spiegel, D. N. et al. 2003, ApJ, in press

Stoughton, C., et al. 2002, AJ, 123, 485

Strauss, M., et al. 2002, AJ, 124, 1810

Szalay, A. S. & Schramm, D. N. 1985, Nature, 314, 718

York, D. G. et al. 2000, AJ, 120, 1579

Zandivarez, A., Merchan, M. E., & Padilla, N. D. 2003, astro-ph/0303450

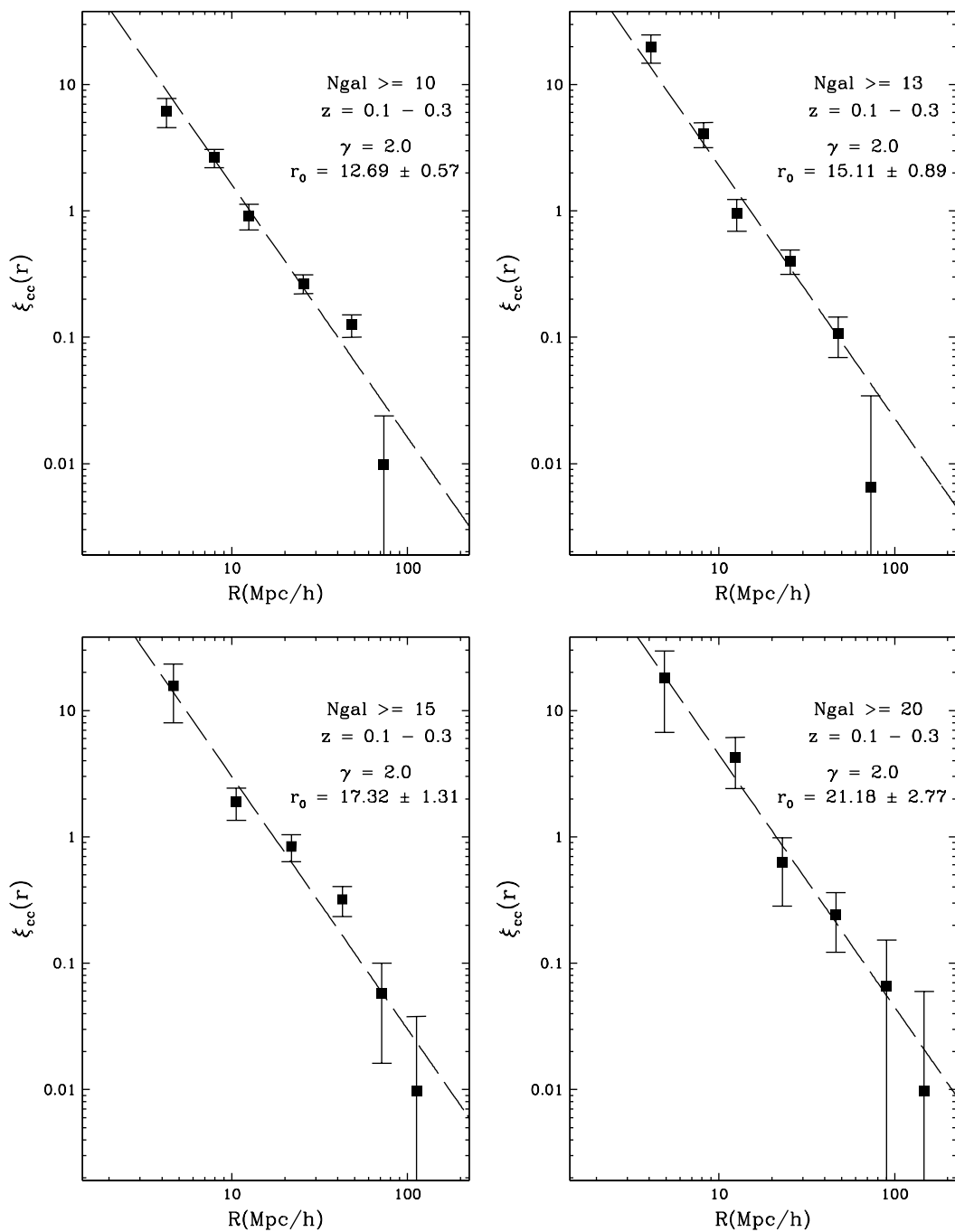


Fig. 1.— The SDSS cluster correlation function for four richness thresholds ($N_{gal} \geq 10$, ≥ 13 , ≥ 15 , ≥ 20). Best-fit functions with slope 2 and correlation-scale r_0 are shown by the dashed lines ($1\text{-}\sigma$ uncertainties).

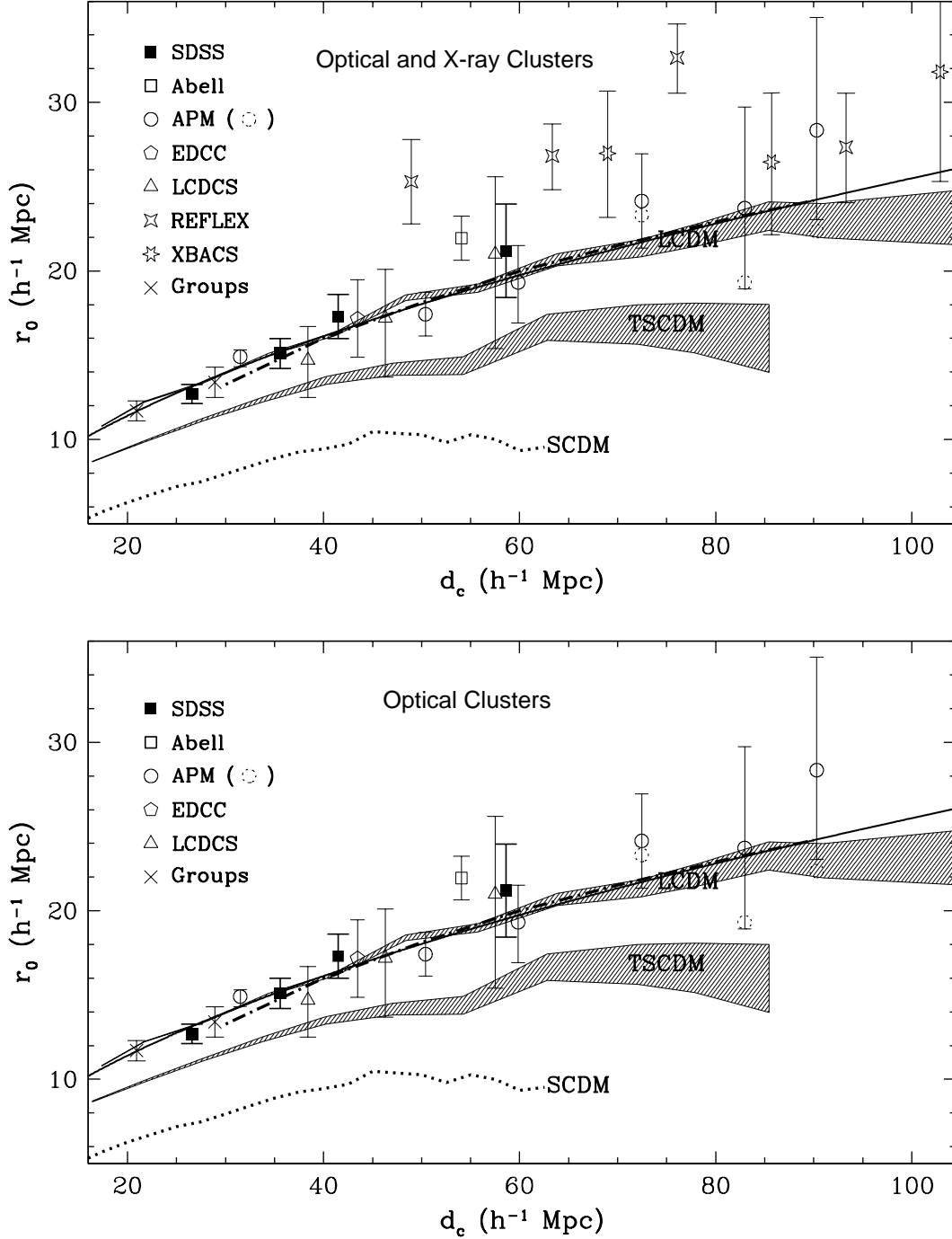


Fig. 2.— Correlation-scale r_0 versus mean cluster separation d for all samples (Fig.2a) and for optical samples (Fig.2b) ($1-\sigma$ uncertainties). A slope $\gamma=2$ and LCDM comoving scales are used (due to conversion to the standard LCDM cosmology, some values differ slightly from Table 1; see §3). Cosmological simulations are presented by the two bands (LCDM and Tilted-SCDM). Previous simulations of LCDM (dot-dash) and untilted SCDM (dotted curve) are also shown (§4). The solid curve represents $r_0 = 2.6\sqrt{d}$ (§4).

Table 1. The Cluster Correlation Function

Sample ^a	N_{cl}	z	γ	r_0 (Mpc)	d (Mpc)
SDSS					
$N_{gal} \geq 10$	1108	0.1-0.3	2	12.7 ± 0.6	26.6
$N_{gal} \geq 13$	472	0.1-0.3	2	15.1 ± 0.9	35.6
$N_{gal} \geq 15$	300	0.1-0.3	2	17.3 ± 1.3	41.5
$N_{gal} \geq 20$	110	0.1-0.3	2	21.2 ± 2.8	58.1
Abell (1,2)					
Rich ≥ 1	195	$\lesssim 0.08$	2	21.1 ± 1.3	52
APM (3)					
R ≥ 50	364	$\sim \langle 0.1 \rangle$	2.1	$14.2 \pm_{0.6}^{0.4}$	30
R ≥ 70	114	$\langle 0.1 \rangle$	2.1	16.6 ± 1.3	48
R ≥ 80	110	$\langle 0.1 \rangle$	1.7	$18.4 \pm_{2.4}^{2.2}$	57
R ≥ 90	58	$\langle 0.1 \rangle$	2.3	22.2 ± 2.8	69
			[2]	$[23.0 \pm 2.9]^b$	
R ≥ 100	29	$\langle 0.1 \rangle$	2.8	18.4 ± 4.8	79
			[2]	$[22.6 \pm 6.0]^b$	
R ≥ 110	17	$\langle 0.1 \rangle$	3.2	21.3 ± 5.3	86
			[2]	$[27.0 \pm 6.7]^b$	
EDCC (4)					
	79	$\lesssim 0.13$	2	16.2 ± 2.3	41
LCDCS (5)					
	178	0.35-0.475	2.15	$14.7 \pm_{2.2}^{2.0}$	38.4
	158	0.35-0.525	2.15	$17.2 \pm_{3.5}^{2.9}$	46.3
	115	0.35-0.575	2.15	$20.9 \pm_{5.6}^{4.6}$	58.1
REFLEX (6)					
$L_X \geq 0.08$	39	$\lesssim 0.05$	2	24.8 ± 2.5	48
$L_X \geq 0.18$	84	$\lesssim 0.075$	2	$25.8 \pm_{2.0}^{1.9}$	61
$L_X \geq 0.3$	108	$\lesssim 0.10$	2	$31.3 \pm_{2.1}^{2.0}$	72
$L_X \geq 0.5$	101	$\lesssim 0.125$	2	$25.8 \pm_{3.3}^{3.2}$	88
XBACS (7,8)					
$L_X \geq 0.24$	49	$\lesssim 0.07$	1.8-2.5	25.7 ± 3.7	66
$L_X \geq 0.48$	67	$\lesssim 0.09$	1.8-2.5	25.2 ± 4.1	82
$L_X \geq 0.65$	59	$\lesssim 0.11$	1.6-2.2	$30.3 \pm_{6.5}^{8.2}$	98
Groups (9)					
$M_v \geq 5e13$	920	$\langle 0.12 \rangle$	2	11.7 ± 0.6	20.9
$M_v \geq 1e14$	540	$\langle 0.13 \rangle$	2	13.4 ± 0.9	28.9

^aSample (with reference), and subsample threshold in richness, X-ray luminosity (10^{44} erg s⁻¹), or M_{vir} (M_\odot). References: 1.Bahcall & Soneira 1983; 2.Peacock & West 1992; 3.Croft et al. 1997; [larger r_0 's are obtained for APM by Lee & Park 1999]; 4.Nichol et al. 1992; 5.Gonzalez, Zaritsky, & Wechsler 2002; 6.Collins et al. 2000; 7.Lee & Park 1999; see also 8.Abadi, Lambas, & Muriel 1998; 9.Zandivarez, Merchan, & Padilla 2003. The SDSS, LCDCS, and Groups use LCDM cosmology for their r_0 and d ; all others use $\Omega_m=1$. All scales are for $h = 1$.

^bCorrelation-scale r_0 using a slope of 2 (see §3)